

DESIGN OF A SMALL PRESSURE CHAMBER TO EVALUATE PROBE CALIBRATIONS AT VARYING REYNOLDS NUMBERS

Konstantin Speck

Research Associate
Technical University of Munich
Chair of Turbomachinery and Flight Propulsion
Email: konstantin.speck@tum.de

Christian Schäffer

Research Associate
Technical University of Munich
Chair of Turbomachinery and Flight Propulsion

Volker Gümmer

Head of Chair
Technical University of Munich
Chair of Turbomachinery and Flight Propulsion

ABSTRACT

This paper describes the design and the validation process of a pressure chamber. The pressure chamber is used to calibrate probes for turbomachinery applications at comparable conditions to a 3.5-stages axial compressor test rig. It allows to study Reynolds number- and Mach number- effects individually.

The Chair of Turbomachinery and Flight Propulsion (LTF) at the Technical University of Munich (TUM) operates a calibration wind tunnel (Caljet). The pressure chamber is designed as an additional component for the calibration tunnel to enable probe calibration at higher mass flow densities and higher Reynolds numbers. Therefore, the original free stream jet is encased by this chamber, nevertheless, the outlet of the calibration wind tunnel is still open to the environment.

After a first pre-design study, numerical simulations are carried out to confirm expected flow conditions in the measurement area. Ansys Fluent is used for RANS simulations with air modeled as compressible gas are carried out. The numerical results are validated with experimental investigations that also give a deeper understanding of the flow behavior. Therefore, a five-hole probe, a hot-wire probe, and a Fast Response Aerodynamic Probe is utilized. It is shown, that the capability of the jet meets the expectations and can be used for the calibration of hot-wire probes at conditions comparable to a state-of-the-art 3.5-stages axial compressor.

NOMENCLATURE

5HP	Five-hole probe
FRAP	Fast Response Aerodynamic Probe
HW	Hot-wire probe
LTF	Chair of Turbomachinery and Flight Propulsion
HSRC	High-Speed Research Compressor
P	Pressure

Ma	Mach number
ρV	Mass flow density
T	Temperature
V	Longitudinal velocity
\bar{v}	RMS of turbulent velocity fluctuations
D	Diameter
L	Length
TI	Turbulent Intensity

SUBSCRIPTS

max	Maximum equivalent value
t	Total value
s	Static value
ref	Reference value

INTRODUCTION

A detailed understanding of the flow physics and aerodynamic loss mechanisms within turbomachinery is still an ongoing challenge. Therefore, probes with a high spatial and temporal resolution are utilized to resolve the flow within LTF's High-Speed Research Compressor (HSRC) at the TUM. The test vehicle is equipped with several traversing slots which enable the investigation of the flow within a modern high-pressure compressor rear stage concept. The applied probes like

- five-hole probes (5HP),
- total temperature and total pressure Kiel-probes,
- Fast-Response Aerodynamic Probes (FRAP),
- and hot-wire probes (HW)

are calibrated under steady conditions in a calibration tunnel concerning yaw and pitch angle, Mach number, and total temperature.

During the calibration of the HW probes a permanent wire breakage occurred when exceeding a certain Mach number, which might be related to wire vibrations, also discovered by Boyle et al. [1] However, the pressure chamber allows to calibrate the HW probes at moderate Mach numbers but at higher mass flow densities by increasing the static pressure inside the chamber. Therefore, the pressure chamber gives the possibility to calibrate a probe at the same steady conditions in terms of Mach number, total temperature, and mass flow density as in the HSRC.

Gieß et al. described in [2] a new test facility for probe calibration, which allows independent variation of Mach and Reynolds numbers. The complex setup and good equipment provide a large working range. This probe calibration wind tunnel is mainly used to calibrate pressure probes.

Furthermore, a preliminary numerical investigation by Schäffer et al. [3] yielded a small dependency of the Reynolds number on the calibration of a five-hole probe. An experimental analysis is necessary to prove the numerical results at lower overpressure. Therefore, this pressure chamber concept is designed to vary the Mach and Reynolds number independently in a range from ambient pressure up to 1250 hPa and Mach numbers from $Ma = 0,05$ to $Ma = 0,9$.

DESIGN

As described before, the pressure chamber is adapted to an existing calibration wind tunnel. The design aims to extend the capability from free stream calibrations to calibrations at higher ambient pressure. Therefore, the pressure chamber is designed with a plug-and-play principle to mount and demount the chamber in a short time.

Wind Tunnel

The existing wind tunnel is a free stream wind tunnel. The air is provided via different systems, depending on the required temperature and Mach number.

For low Mach numbers and no temperature dependence, two different Blowers can be used, depending on the required Mach number. Higher Mach numbers are realized with the 13 bar shop air supply that has sufficient large compressors and pressure tanks. Since rising the ambient pressure goes hand in hand with throttling up the pressure chamber, all investigations with the pressure chamber require the 13 bar pressure system. The simplified schematic setup is shown in Figure 1.

An electronic valve is used to control the supply pressure from the pressure system. The 18 kW Heater heats up the flow by $\Delta T_{\text{Heater}} = 100$ K at a mass flow up to $\dot{m}_{\text{max heater}} = 0.2$ kg/s and a maximum pressure of 1250 hPa.

The settling chamber has a diameter of $D_{\text{settling chamber}} = 500$ mm and a length of $L_{\text{settling chamber}} = 1000$

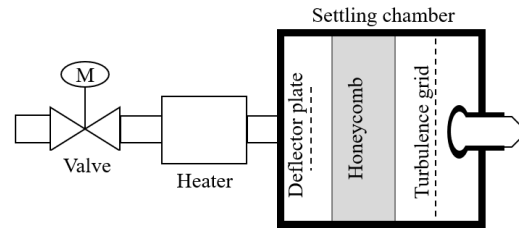


Figure 1. Setup of existing wind tunnel

mm. It is isolated with a 3 cm thick high-temperature resistant isolation material. To generate a homogenous flow field a deflector plate, honeycomb, and a screen are placed inside the settling chamber.

After a throat, a nozzle is mounted that accelerates the flow to the required Mach number. Depending on the probe head dimensions, three different nozzle sizes are available with a diameter of $D_{\text{Nozzle}} = 25$ mm, 35 mm, and 42 mm. Therefore, small probes can be calibrated with the 25mm nozzle up to very high Mach numbers still with the blower that enables easier control of the flow velocity.

Around the nozzle, a traversing system is installed to rotate the probes for an unlimited yaw angle and a pitch angle range of $\pm 45^\circ$.

Pressure Chamber

The existing free stream calibration tunnel is adapted, to become a closed measuring section calibration tunnel. To allow the calibration of hot-wire probes, an exact knowledge of the total temperature is necessary. Therefore, a second probe slot for a total temperature Kiel probe next to the slot for the HW is required. Eckelmann showed in [4], that the static pressure in flow direction is changing due to a change in the boundary layer thickness, which has to be considered. Further requirements are, to set up a design that can be used via remote, is automated as far as possible, and has sufficient safety controls.

The propagated design is shown in Figure 2.

The pressure chamber has an inner diameter of $d_{\text{in}} = 150$ mm. The length between the nozzle outlet until the contraction area is defined as $L_{\text{pressure chamber}} = 180$ mm.

The contraction area creates a transition from the $D = 150$ mm diameter to $D = 75$ mm with a 20° angle which is necessary to connect the chamber to the following downstream tubing and the throttle valve.

The measuring positions of the static pressure is located in 10 mm steps from -10 mm to 80 mm in axial position relative to the outlet of the nozzle. The average over two circumferential positions for each

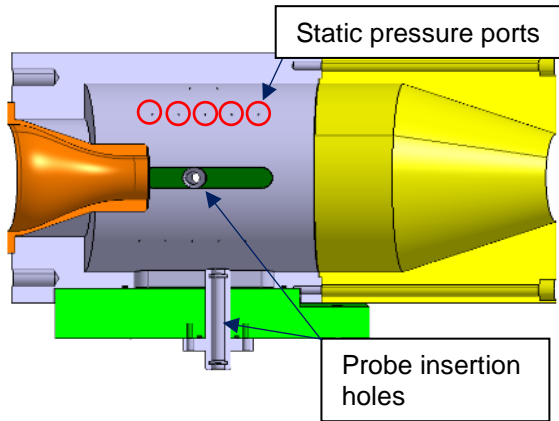


Figure 2. Design inside the pressure chamber

axial position is used for the static pressure measurement. At the axial positions, 30 mm and 50 mm downstream of the nozzle, where the main calibration area is located, even three circumferential distributed measurement points for the static pressure are available.

Up to two probes can be placed in parallel between the nozzle outlet and 80 mm downstream of the nozzle. For each axial position, an individual mounting plate has to be manufactured to ensure proper sealing. During HW probe calibrations a T_r-Kiel probe is mounted off-center and slightly shifted behind the HW probe, to prevent any influence from the potential field of the Kiel probe on the HW (cf. Figure 3).



Figure 3. Two probes mounted in the pressure

Figure 4 illustrates the whole pressure chamber setup. The components are described as follows. A vertical slide with a rotational table (2) enables free movement in the yaw and radial direction. An automated variation of the pitch angle is not possible, since the small design doesn't allow a sealing for higher pressures while pitching. Therefore, one can insert between the mounting plate (4) and the pressure chamber (1) a wedge that tilts the plate, providing a certain pitch angle. To ensure the sealing between the pressure chamber and the probe, a probe guidance (3) is manufactured

where the probe is slid through. Two O-rings at the top and the lower side are sealing the guidance to the probe. For every probe diameter, a probe guidance has to be manufactured. Probes with a diameter of up to 12 mm can be used in the pressure chamber. After the outlet of the pressure chamber, a two-meter-long metal tube is mounted to settle the flow (not shown in the picture). A tee (6) is placed downstream of the conditioning tube. On one side, a manual valve (5) is placed for a coarse adjusting of the degree of throttling and also to prevent the calibration tunnel from overpressure in case the electric valve (7) has a malfunction and closes completely.

The electric control valve (7) is placed to allow a full remote capability and also a precise adjustment of the mass flow.

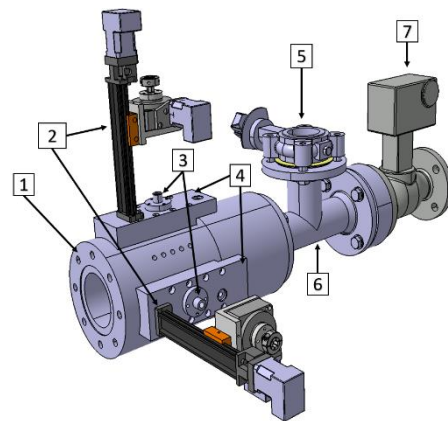


Figure 4. Pressure chamber configuration

NUMERICAL INVESTIGATION

A numerical simulation is carried out to confirm that the measurement area is not influenced by any effects of the geometry of the pressure chamber.

Ansys Fluent 2021 R2 in combination with Fluent Meshing is used for the simulations. All simulations are conducted on a local workstation with 16 physical cores.

Small simplifications to the geometry are done in areas not affecting the main flow, e.g. the cavities for inserting the probe are not modeled.

The inlet boundary condition is defined by the total pressure and total temperature. The outlet boundary condition is set by the mass flow. The outlet is moved in axial direction to get better conditioning of the flow and stabilize the numerical simulation.

The SST-Turbulence-model is used, air is defined as a compressible ideal gas and the energy equation is resolved.

A mesh independency study yields that a mesh with 11 Mio. cells is of adequate size to get reliable results. The flow at the walls is resolved and the

maximal y^+ value is 1,2. The overall calculation time is about 11 h.

The aim of the simulation is to check the behavior of the main flow. Table 1 gives an overview of the simulation settings.

Table 1. Numerical boundary conditions

Turbulence Model	SST
Ambient pressure	96450 Pa
Inlet total pressure (relativ)	80224 Pa
Inlet total temperaure	293 K
Inlet turbulent intensity	0.8 %
Outlet mass flow	0,2223 kg/s
Nozzle diameter	35 mm
Fluid	Air
Density	Compressible, ideal gas

Figure 5 is showing the Mach number distribution in the axial-radial plane. It can be seen, that the main flow is not deflected by the pressure chamber.

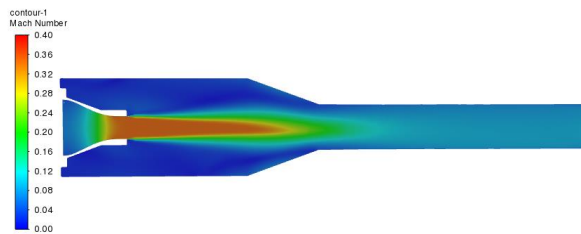


Figure 5. Distribution of Mach number in numerical

EXPEIMENTAL INVESTIGATION

To validate the numerical results, experimental investigations are carried out.

The regulation of the flow conditions is very complex since a change in the static pressure by throttling up the pressure chamber with (5) and (7) in Figure 4 also induces a decrease in the Mach number and v . Therefore, the blower or the valve in Figure 1 needs to be adjusted which again changes the conditions inside the pressure chamber. Additionally, a change in the flow temperature with the heater also causes deviations. This requires an iterative procedure until the desired Mach number, mass flow density, and temperature are finally set.

The following results show data of the probe installed at 30.9 mm behind the outlet of the nozzle.

At first, the flow with and without the pressure chamber mounted at the Caljet is compared for a completely unthrottled flow. The tests without the pressure chamber are conducted with only the blue-grey part in Figure 2 installed, to keep the probe in the exact same position and to obtain the exact same traversing capabilities.

Turbulence Measurement

Table 2 shows the Turbulent Intensity (TI) for tests with and without pressure chamber measured with HW and FRAP. The TI calculated via HW is based on the principle presented by Boufidi et al. [5]:

$$TI = \frac{\sqrt{\overline{v'^2}}}{\bar{v}}$$

\bar{v} is the mean velocity of the flow in flow direction since a single wire is utilized. $\sqrt{\overline{v'^2}}$ represents the square root of the variance hence the root-mean-square of the velocity fluctuations.

The Turbulence Intensity measured with a 2-Sensor-FRAP is calculated in accordance with the approach from Hinze [6].

As seen in Table 2, for all tests the TI is in good agreement for all methods. Only the TI for the FRAP measurements using the pressure chamber is slightly higher. It has to be considered, that the uncertainty for calculating the TI from the FRAP data is higher. Nevertheless, the overall TI is relatively high for a probe calibration wind tunnel due to the geometry and small number of screens in the settling chamber.

Table 2. Turbulent Intensity at $Ma=0.4$

	Turbulent Intensity [%]
FRAP without pressure chamber	0.80
FRAP with pressure chamber	0.97
HW without pressure chamber	0.80
HW with pressure chamber	0.80

Comparison w/ and w/o Pressure Chamber

Figure 6 illustrates the mass flow density measured with the FRAP with and without the pressure chamber installed. The tests were carried out at different days with a significantly different ambient pressure. Therefore, the mass flow density is presented in a normalized manner.

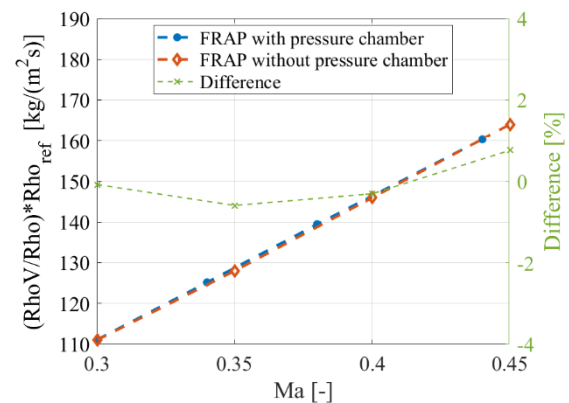


Figure 6. Mass flow density of FRAP over different Mach numbers

Figure 7 shows that the differences in the Mach number with and without the pressure chamber is below 1%. The difference of the Mach number of around $\Delta Ma \approx 0.003$ is comparable to results from Gieß et al. in [2].

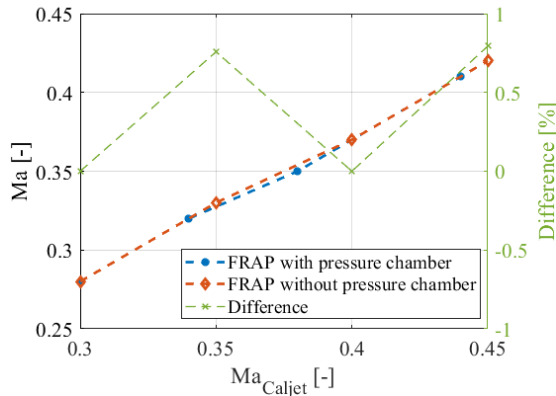


Figure 7. Measured Mach number of FRAP over different Mach numbers of Caljet

Flow Distribution behind Nozzle

Figure 8 shows the CFD prediction of the nozzle profile of the Mach number compared to experimental results at throttled conditions. The flow condition is kept stable at a defined static pressure and Mach number. During the test, the pressure distribution inside the flow is measured with a 5HP. The mass flow is set as boundary condition for the simulation and is calculated from experimental data. The total and static pressure is measured with an accuracy of ± 25 Pa and the total temperature with an accuracy of ± 1.5 K. This error is leading to a difference in the measured mass flow from -0.5% to +0.17 %.

It can be seen, that the behavior of the main flow between simulation and experimental data agrees very well. Additionally, the Mach number calculated from the total pressure inside the settling chamber and the static pressure inside the pressure chamber agrees very well with the Mach number from the 5HP.

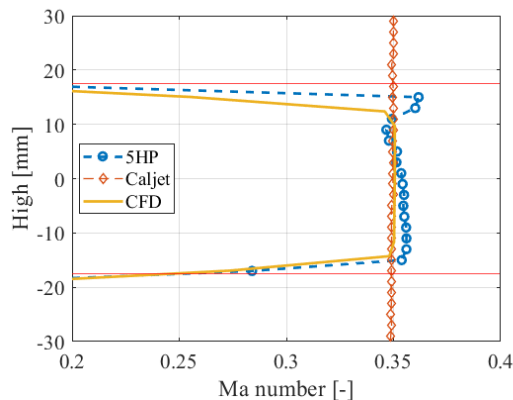


Figure 8. Mach number distribution inside the pressure chamber after the nozzle

Figure 9 illustrates the pressure distribution inside the pressure chamber. The pressure is normalized by the total pressure inside the settling chamber. The 5HP data agrees very well with the measured values from the Caljet. But the 5HP data is not reliable in the shear area around the main flow, since the strong velocity gradient leads to problems also observed by Willinger et al. in [7]. A slight shift of the static pressure measured by the 5HP compared to the static pressure of the Caljet can be noticed.

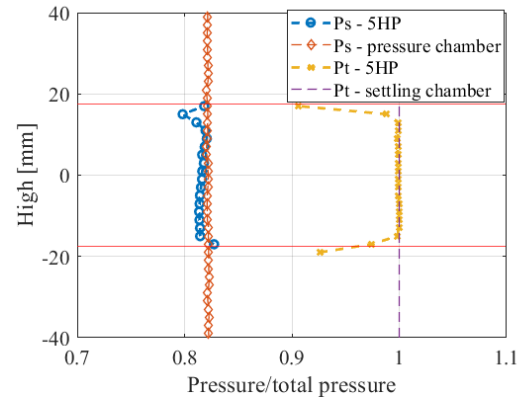


Figure 9. Pressure distribution inside the pressure chamber after the nozzle

Tests at throttled flow conditions

Figure 10 represents the mass flow density measured with the HW over the static pressure. While the Mach number is kept constant at $Ma=0.4$, the pressure chamber is throttled up. The linear behavior between static pressure and mass flow density can be observed.

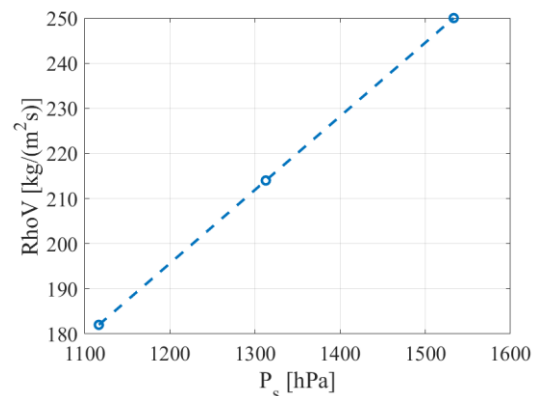


Figure 10. Mass flow density inside the pressure chamber at $Ma=0.4$

Additional tests are carried out to check the throttling system. Therefore, a certain level of throttling is applied while the total pressure is varied. A 5HP is placed 30,9 mm downstream of the nozzle.

Figure 11 shows the mass flow density over the ratio of the static pressure P_s to the ambient pressure P_{amb} . The static pressure inside the pressure chamber is raising up to 1.38 times the ambient pressure. The mass flow density of the 5HP is calculated with the temperature measured in the settling chamber. Usually the total temperature Kiel probe after the nozzle is used for measuring the flow temperature as a significant heat exchange over the throat and nozzle leads to a wrong temperature measurement inside the settling chamber. But since the flow temperature is close to the ambient temperature and stays quite stable by using the 13 bar pressure system and even does not change for different Mach numbers, this assumption is valid. It can be seen, that the measured mass flow density from the 5HP has only small deviations compared to the mass flow density measured by the Caljet.

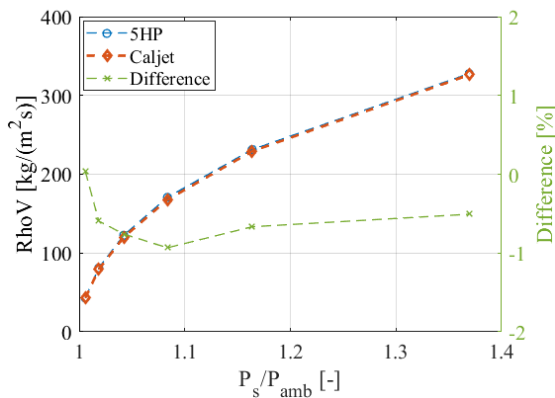


Figure 11. Mass flow density at varying total pressure

Figure 12 shows the total pressure at different static pressure levels inside the pressure chamber. The measured values from the Caljet and 5HP agree very well, also for different Mach numbers.

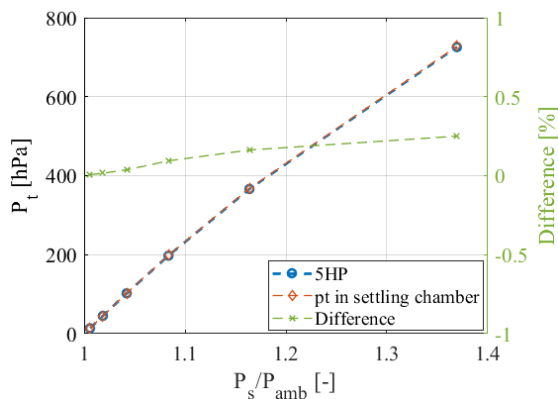


Figure 12. Total pressure at different pressure levels inside the pressure chamber

Capability of Pressure Chamber Configuration

Figure 13 and Table 3 illustrate the capability of the calibration wind tunnel in combination with the pressure chamber. The maximum Reynolds number for different Mach numbers and temperatures is shown. The maximum mass flow density of $Rho V_{max}=480 \text{ kg/(m}^2\text{s)}$ is reached at $Ma=0.9$ and a Temperature of $T=293 \text{ K}$.

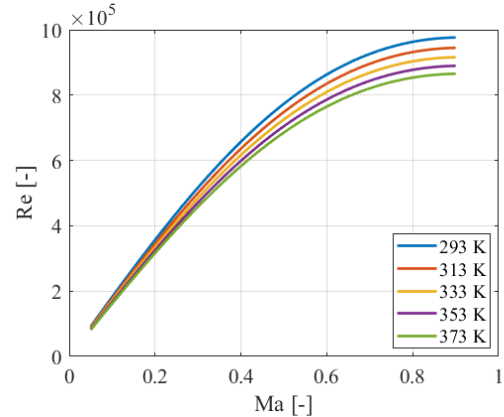


Figure 13. Capability of calibration wind tunnel with pressure chamber

Table 3. Calibration tunnel capability

	Value	Unit
Mach number	0.02-0.95	-
Calibration static pressure (depending on required Mach number)	amb – 1250	hPa
Maximum total pressure	1250	hPa
Nozzle diameter	25, 35, 42	mm
Temperature	293 – 373	K
Mass flow density	22 - 480	kg/m ² s
Nozzle Reynolds number	$8 \times 10^4 - 9 \times 10^5$	-

Safety

Since neither the settling chamber nor the pressure chamber is rated for a pressure of 13 bar, a safety mechanism is required. Therefore, two overpressure valves are installed at the settling chamber. Furthermore, during operations including the pressure chamber, it is not allowed to close the manual throttling valve completely (cf. Figure 4 (5)).

OUTLOOK AND DISCUSSION

At the Chair of Turbomachinery and Flight Propulsion at the Technical University of Munich a modification for varying the Reynolds number independent from the Mach number, of an existing probe calibration wind tunnel, is introduced. The design of a pressure chamber including a throttling system is described. The capability and quality of the design is investigated via numerical simulations

and experimental tests. The results show that neither the throttling mechanism nor the pressure chamber itself is influencing the calibration area where the probe is located.

The new pressure chamber has the capability to conduct calibrations of HW probes at temperatures between 291 K and 373 K, with a mass flow density from 22 kg/(m²s) to 480 kg/(m²s). The Mach number can be varied from Ma = 0.05 to Ma = 0.9.

The pressure chamber is used to calibrate HW probes at equal conditions compared to a 3.5-stages axial compressor concept.

For further investigations regarding higher static pressures, the pressure chamber will be adapted to a different calibration wind tunnel with a higher pressure rating. Furthermore, the connection to the pressure sensors will be changed, to gain a higher pressure ratio capability and to review the numerical results from Schäffer et al. in [3] over the whole numerical pressure range.

REFERENCES

- [1] Boyle, R. J.; Lucci, B. L.; Senjitko, R. G.; Aerodynamic Performance and Turbulence Measurements in a Turbine Vane Cascade; *ASME TURBO EXPO 2002*; GT-2002-30434
- [2] Gieß, P.-A.; Rehder, H.-J.; Kost, F.; A New Test Facility for Probe Calibration - Offering Independent Variation of Mach and Reynolds Number; *XVth MTT, 2000*
- [3] Schäffer, C.; Speck, K.; Gümmer, V.; Numerical calibration and investigation of the influence of Reynolds number on measurements with five-hole probes in compressible flows; *ASME Journal of Turbomachinery* 9/2022; DOI: 10.1115/1.4053835
- [4] Eckelmann, H.; Einführung in die Strömungsmechanik, DOI 10.1007/978-3-663-09882-9
- [5] Boufidi, E.; Lavagnoli, S.; Fontaneto, F.; A Probabilistic Uncertainty Estimation Method for Turbulence Parameters Measured by Hot-Wire Anemometry in Short-Duration Wind Tunnels; *ASME Journal of Engineering for Gas Turbines and Power* 3/2020; DOI: 10.1115/1.4044780
- [6] Hinze, J. O.; Turbulence; McGraw-Hill, 1975, ISBN-13: 978-0070290372
- [7] Willinger, R.; Haselbacher, H.; A Three-Hole Pressure Probe Exposed to Velocity Gradient Effects – Experimental Calibration and Numerical; *Conference on Modelling Fluid Flow 9/2003*; DOI: 10.1115/1.4044780